THE JOURNAL OF PHYSICAL CHEMISTRY B

ARTICLE

pubs.acs.org/JPCB

Comparing the Temperature Dependence of Photosynthetic Electron Transfer in *Chloroflexus aurantiacus* and *Rhodobactor sphaeroides* Reaction Centers

Zhi Guo,[†,#] Su Lin,[†,¶] Yueyong Xin,[‡,§] Haiyu Wang,[†,∥] Robert E. Blankenship,[‡] and Neal W. Woodbury*[,†,▽]

[†]The Biodesign Institute at Arizona State University, Arizona State University, Tempe, Arizona 85287-5201, United States

[‡]Departments of Biology and Chemistry, Washington University in St. Louis, St. Louis, Missouri 63130, United States

[#]Department of Physics, Arizona State University, Tempe, Arizona 85287-1504, United States

[¶]Department of Chemistry and Biochemistry, Arizona State University, Tempe, Arizona 85287-1604, United States

[▽]Department of Chemistry and Biochemistry, Arizona State University, Tempe, Arizona 85287-1604, United States

Supporting Information

ABSTRACT:

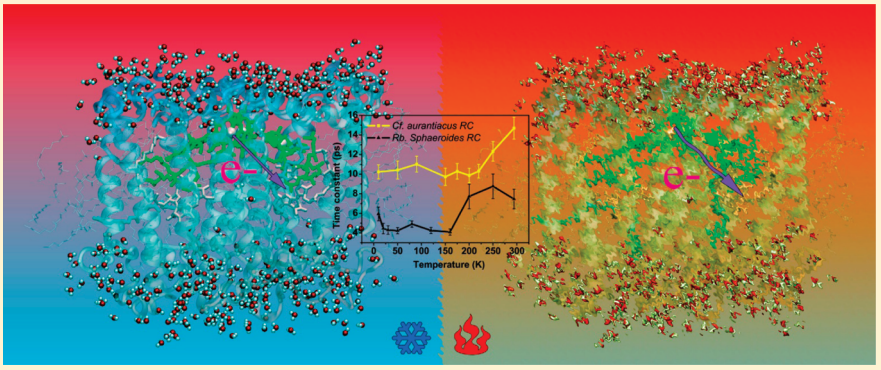

The process of electron transfer from the special pair, P, to the primary electron donor, H_A, in quinone-depleted reaction centers (RCs) of *Chloroflexus (Cf.) aurantiacus* has been investigated over the temperature range from 10 to 295 K using time-resolved pump−probe spectroscopic techniques. The kinetics of the electron transfer reaction, $P^* \rightarrow P^+H_A^-$, was found to be nonexponential, and the degree of nonexponentiality increased strongly as temperature decreased. The temperature-dependent behavior of electron transfer in *Cf. aurantiacus* RCs was compared with that of the purple bacterium *Rhodobacter (Rb.) sphaeroides*. Distinct transitions were found in the temperature-dependent kinetics of both *Cf. aurantiacus* and *Rb. sphaeroides* RCs, at around 220 and 160 K, respectively. Structural differences between these two RCs, which may be associated with those differences, are discussed. It is suggested that weaker protein−cofactor hydrogen bonding, stronger electrostatic interactions at the protein surface, and larger solvent interactions likely contribute to the higher transition temperature in *Cf. aurantiacus* RCs temperature-dependent kinetics compared with that of *Rb. sphaeroides* RCs. The reaction-diffusion model provides an accurate description for the room-temperature electron transfer kinetics in *Cf. aurantiacus* RCs with no free parameters, using coupling and reorganization energy values previously determined for *Rb. sphaeroides*, along with an experimental measure of protein conformational diffusion dynamics and an experimental literature value of the free energy gap between P* and $P^+H_A^-$.

INTRODUCTION

Protein folding studies have demonstrated the importance of the protein conformational energy landscape in determining the pathway and products of the protein folding process.[1,2] Given this, it is perhaps not surprising that conformational dynamics of fully folded protein systems play a critical role in native protein function. While this concept is not new, the past decade has seen a dramatic increase in the number and sophistication of theoretical and experimental studies in this area. This work includes increasingly accurate calculations from simulation studies,[3−6] the observation of conformational fluctuation associated with the function at the single molecule level[7−9] and a variety of studies of photoinitiated chemical processes in proteins,[10−13] such as those that employ ultrafast X-ray diffraction techniques.[14−16]

One of the most important realizations that has emerged from this work is that dynamic heterogeneity is not a liability to protein systems, but is likely pivotal in making them as functionally robust as they are. The ability to explore local conformational space means that moderate changes in the environment, or even in protein sequence, can be accommodated by maintaining a level of conformational

Received: May 6, 2011
Revised: August 9, 2011
Published: August 09, 2011

flexibility that allows the protein to compensate appropriately. An important aspect of this adaptability is that proteins undergo conformational changes over a very broad range of time scales, from femtoseconds to hours, making them an extremely versatile solvent for performing chemistry and ensuring that movement, and the associated changes in the energy landscape of the system, occurs on essentially any time scale relevant to biology.

Different experimental approaches have been used to look at reactions on various time scales. However, in the subnanosecond regime, where essentially all electron transfer reactions take place, spectroscopic measurements of photoinduced charge separation and associated protein movement dominate. In this regard, the photosynthetic reaction center (RC) of purple nonsulfur photosynthetic bacteria is perhaps the best characterized system. This protein–pigment complex uses light energy to power a series of electron transfer reactions that ultimately yield a charge-separated state that drives trans-membrane proton translocation. In recent years, it has become evident that electron transfer in this system is directly dependent on protein dynamics. In other words, the exploration of protein conformational space is rate limiting in photosynthetic electron transfer, and thus it is this conformational diffusion that actually determines charge separation kinetics. This type of electron transfer kinetics is embodied in the concept of reaction diffusion in polymer systems and, as a model for nonergodic reactions, does an excellent job of describing the electron transfer kinetics of bacterial RCs over a broad range of temperatures and reaction free energies.

One of the great advantages of studying bacterial photosynthetic RCs is their robust nature; isolated RCs are stable for long periods at room temperature and can undergo many cycles of photoexcitation. In addition, their structure is easily altered through genetic modification, and they are very tolerant of mutational change in terms of protein folding and cofactor assembly. By taking advantage of these characteristics, a great deal has been learned about the role of thermodynamics in RC function and in the mechanistic details of specific cofactor function in electron transfer. However, exploring the role of protein conformational dynamics is more difficult. It is hard to imagine how one would systematically alter the distribution and interconversion of different RC conformations via mutagenesis. Fortunately, nature has provided examples of proteins in which the conformational flexibility been altered in more or less predictable ways. Thermophilic proteins are stable at high temperature in part because they limit access to protein conformations that could lead to denaturation or loss of function. There are a number of thermophillic photosynthetic bacterial systems available, and analysis of these RCs, in comparison to mesophilic RCs, may provide an avenue for probing the effects of systematic changes in conformational diffusion on electron transfer. In particular, one might expect that both the rate of conformational interconversion and its temperature dependence should be altered in thermophilic versus mesophilic proteins. Here, this concept is explored through a detailed comparison of the electron transfer kinetics of the RCs of *Rhodobacter (Rb.) sphaeroides*, a mesophilic, purple nonsulfur bacterium, and *Chloroflexus (Cf.) aurantiacus*, a thermophilic, filamentous anoxygenic phototroph (FAP).[17,18]

The structure of RCs from *Rb. sphaeroides* is well-known in multiple forms and includes 10 cofactors: four bacteriochlorophyll (BChl) molecules, two bacteriopheophytin (BPheo) molecules, two ubiquinone molecules, a carotenoid molecule, and a nonheme iron atom. These cofactors are bound to two symmetrically related protein subunits, L and M, and form two symmetrically arranged electron transfer chains (referred to as A and B, Figure 1A). A third protein subunit, H, is located on the cytoplasmic membrane side of the complex. In isolated wild-type RCs, only the cofactors in the A-branch appear to be actively involved in the primary electron transfer reactions and each of the reaction steps has been well-characterized spectroscopically.[19] The initial charge separation occurs from the excited state of the two closely coupled BChls P (P*) to a BChl monomer (B_A), forming the state $P^+B_A^-$ in 3 ps. The electron is then transferred from B_A^- to the BPheo (H_A), and finally to the quinone (Q_A) with time constants of 0.9 and 200 ps, respectively.

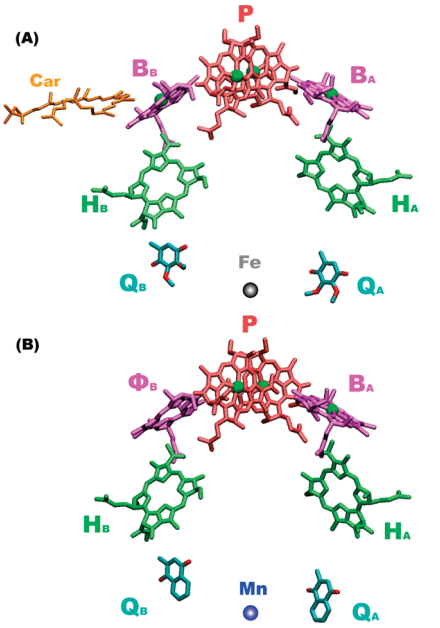

Figure 1. Cofactor arrangement in two bacterial RCs. From top to bottom, red for the BChl dimer (P), magenta for BChl monomer (B, or for B branch in *Cf. aurantiacus* RC, Φ is used), green for bacteriopheophytin (H), cyan for quinones (Q), and metals between two quinones (Fe for *Rb. sphaeroides*, Mn for *Cf. chloroflexus*) at the bottom. Carotenoid (Car) in *Rb. sphaeroides* RC is in orange color. (A) *Rb. sphaeroides* RC, (B) *Cf. chloroflexus* RC. The cofactor arrangement for the *Rb. sphaeroides* RC is obtained from ref 61(PDB ID: 1PRC), the cofactor arrangement for *Cf. chloroflexus* RC is a "schematic" illustration modified from the *Rb. sphaeroides* RC. Graphs were prepared by VMD software.

The structure of the RC from *Cf. aurantiacus* has not yet been determined, but past studies have suggested that its form and function is similar to that of *Rb. sphaeroides*,[20] although the two organisms are phylogenetically quite separate.[21] A schematic model of the cofactor composition of the *Cf. aurantiacus* RC, based on the structure of the *Rb. sphaeroides* RC, is shown in Figure 1B. While the *Cf. aurantiacus* RC contains L and M protein subunits that are the functional analogues of those found in *Rb. sphaeroides*, it lacks the H protein subunit.[18] Comparing cofactors between the two types of RCs reveals that the monomeric BChl in the B-branch of the *Rb. sphaeroides* RC is a BPheo molecule in the *Cf. aurantiacus* RC, the carotenoid near B_B is missing, and the *Cf. aurantiacus* RC utilizes menaquinone, instead of ubiquinone, as the secondary electron acceptor.[18] In addition, there are some key differences in amino acid residues between the L and M protein subunits of *Cf. aurantiacus* and *Rb. sphaeroides* RCs that likely affect the cofactor properties.[21]

In *Cf. aurantiacus* RCs, the ground state absorption band of P peaks at 865 nm, similar to that in *Rb. sphaeroides* RCs.[18] It red-shifts to 887 nm at 77 K and remains at roughly the same position down to 4 K. The stimulated emission from P* has been studied

in *Cf. aurantiacus* RCs in polyvinyl alcohol films as a function of temperature, and the time constant of the initial electron transfer ($P^* \rightarrow P^+H_A^-$) was found to be 7.0 ps at room temperature, becoming biexponential (3.0 and 32 ps) at 80 K.[22] The corresponding overall electron transfer rates in *Rb. sphaeroides* RCs are 3 and 1.5 ps at room temperature and 77 K, respectively, when a single time constant is assumed;[23,24] although more detailed studies make it clear that the reaction is really kinetically heterogeneous. For example, using two components to describe the kinetics results in components of roughly 2 and 10 ps with the 10 ps component having a 10−20% amplitude at room temperature.[25] In *Rb. sphaeroides*, the kinetic heterogeneity appears to decrease with decreasing temperature, so that at 10 K, the reaction is essentially single exponential. Kirmaier et al. have investigated $P^+Q_A^-$ formation kinetics and determined the time constant to be 365 ± 19 ps in *Cf. aurantiacus*, which is slower than that found in *Rb. sphaeroides* RCs (~200 ps).[26] Volk et al. analyzed the $P^+H_A^-$ charge recombination process and determined that the energy gap between the P* state and the $P^+H_A^-$ state in *Cf. aurantiacus* RCs is about 0.04 eV less than that in *Rb. sphaeroides* RCs.[27] Recent studies by Collins et al. on RCs from *Roseiflexus castenholzii*, an organism closely related to *Cf. aurantiacus*, have produced generally similar results.[28]

In this study, we measured the temperature-dependent electron transfer kinetics of *Cf. aurantiacus* RCs in detail over a wide temperature range (10−294 K). The results were compared with those of *Rb. sphaeroides* RCs, which contains the same cofactors involved in the initial electron transfer reactions, except for a protein environment evolved for mesophilic rather than thermophilic function.

MATERIALS AND METHODS

Sample Preparation. Q_A-containing RCs of *Cf. aurantiacus* were prepared using a protocol previously described.[29] To remove quinones, isolated RCs were loaded on a Q-sepharose HP 5 mL column and washed extensively with 1 L of 0.2% Triton X-100 (reduced form) in 20 mM Tris-HCl buffer (pH 8.0) until the absorbance (260−960 nm) returned to its baseline value. This concentration of Triton X-100 is sufficient to remove quinones in more than 99% of the *Chloroflexus* RCs. The quinone-depleted RCs were then eluted in the same buffer plus 100 mM NaCl. The peak fractions contained RCs with A_{860} greater than 10 in a 1-cm cuvette. The resulting samples were diluted with 0.1% lauryldimethylamine oxide (LDAO) in Tris buffer (20 mM, pH8.0) to a final OD of 0.6 at 860 nm in the 1.2 mm optical path-length measuring cell.

Spectroscopic Measurements. Femtosecond transient absorption spectroscopy was carried out using a pump−probe setup described previously.[30,31] Laser pulses were generated at a repetition rate of 1 kHz with 130 fs duration at 800 nm using a regenerative amplifier system based on a Titanium:Sapphire laser (Millennia, Tsunami, Spitfire, Spectra-Physics Lasers). Part of the beam was used to pump an infrared optical paramagnetic amplifier (OPA-800, Spectra-Physics) to generate excitation pulses at 860 nm, and the other part was focused on a sapphire plate to generate a white light continuum that was used as the probe light. Tryptophan kinetics were measured using excitation at 800 and 280 nm probe pulses obtained via second harmonic generation using 560 nm pulses from the OPA. After passing through the sample, the probe pulses were sent through a monochromator (SP150, Action Res. Corp.) and detected by a photodiode detector (Model 2032, New Focus, Inc.). Time-resolved spectra were recorded by scanning the monochromator over the desired wavelength region at a fixed time delay

Kinetic Data Analysis. Both multiple exponential and stretched exponential (Kohlrausch−Williams−Watts function) fitting methods were employed to fit kinetic decay curves. The latter has been widely applied to characterize complex kinetic processes, especially for the analysis of time-dependent photonic spectra and dielectric responses. The time-dependent, stretched exponential function has two nonlinear parameters per component:

$$f(t) = e^{-\left(\frac{t}{\tau}\right)^{\beta}} = \int_0^{\infty} e^{-\frac{t}{\tau}} \rho(\tau)\, d\tau$$

Here, τ is the characteristic time constant in the relaxation distribution, and the index, β, is associated with the width of the distribution, or the variety of the relaxation processes. If β equals ~1, the decay process distribution approaches a Dirac function and the decay becomes essentially single exponential. When β decreases, the distribution of exponential decay times becomes broader, and the average lifetime produced by such a distribution is

$$\langle \tau \rangle = \beta\tau \cdot \Gamma(\beta)$$

where $\Gamma()$ is the gamma function. To extend its application to the simultaneous relaxation of multiple processes, the sum of several stretched-exponentials can be used:

$$f(t) = \sum_i A_i e^{-\left(\frac{t}{\tau_i}\right)^{\beta_i}}$$

Applying the Reaction Diffusion Model to Describe *Cf. aurantiacus* Kinetics. The kinetics of initial electron transfer in RCs of *Rb. sphaeroides* have previously been successfully modeled using a reaction diffusion formalism, as previously described in ref 30 and in the Supporting Information. For the calculations described here, the electronic coupling strength (J) was assumed to be the same in *Cf. aurantiacus* as determined previously for *Rb. sphaeroides*,[30] and the driving force and time-dependent diffusion term were determined from experimental data, as described below.

RESULTS

Initial Electron Transfer Processes and Tryptophan Absorption Kinetics in *Cf. aurantiacus* RCs at Room Temperature. For the temperature-dependent studies described below, it was necessary to remove Q_A from the *Cf. aurantiacus* RCs. These two samples, the Q_A-containing and the Q_A-depleted RCs, were compared both spectrally and kinetically to ensure that there were no major changes in the initial reactions simply due to quinone removal. Both the early time kinetics and spectra were essentially identical, with the initial electron transfer reaction occurring in both cases with biexponential kinetics involving exponential components of roughly 3 and 10 ps (Supporting Information, Figures S1a and S2). Similar kinetics are observed in the Q_Y region of the spectrum, monitoring the ground-state bleaching of H_A and the formation of H_A^- at 540 and 660 nm, respectively (Supporting Information, Figure S3a,b). This is consistent with previous measurements of quinone-containing RCs of *Cf. aurantiacus*.[22,32] As expected, removing Q_A does not strongly affect either the spectra or the kinetics of initial electron transfer, indicating that quinone binding/removal has only a minor influence on the environment of P, as has been seen previously in *Rb. sphaeroides* RCs.[24,33,34] In quinone-containing RCs from *Cf. aurantiacus*, the state $P^+H_A^-$ decays in about 300 ps at room

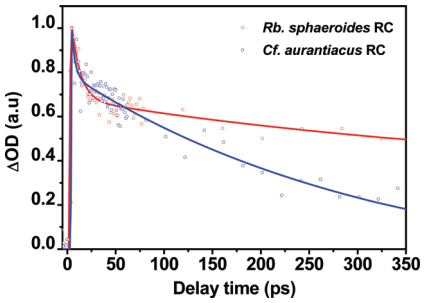

Figure 2. Room-temperature tryptophan absorption change kinetics probed at 280 nm. Red open circles represent Q_A-depleted *Rb. sphaeroides* RCs, and blue open circles represent Q_A-depleted *Cf. aurantiacus* RCs. Smooth curves are the results of a three-exponential fit.

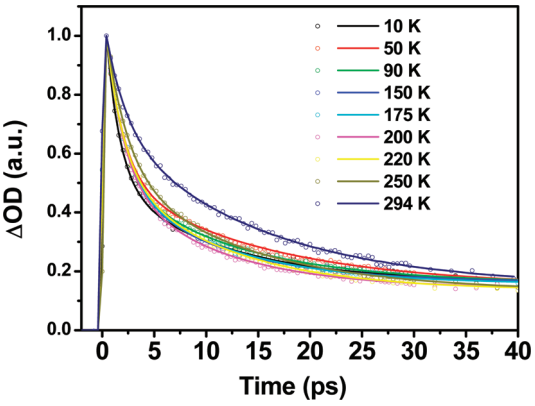

Figure 3. Temperature dependence of the P* decay kinetics in *Cf. aurantiacus* RC over the first 40 ps, probed at 930 nm (signal is inverted for clarity).

temperature as the electron is transferred from H_A to Q_A, in agreement with previous results.[26] Upon removal of the quinone, as expected,[27] the $P^+H_A^-$ lifetime lengthens, decaying on the nanosecond time scale (data not shown).

Previously, the transient absorbance signal from tryptophan has been used to monitor the general kinetics of protein motion in the vicinity of the electron transfer reaction in *Rb. sphaeroides* RCs.[30] A key issue in this work is to understand if the distribution of protein dynamics differs in the thermophillic *Cf. aurantiacus* RC. The change of the tryptophan absorption signal was measured at 280 nm upon special pair excitation, as was done previously in *Rb. sphaeroides* RCs. The induced absorption signal near 280 nm in *Rb. sphaeroides* RCs appears to originate, at least in part, from tryptophans W156(L) and W185(M), which are symmetrically arranged about 7−9 Å from the magnesium centers of the BChls forming P. Alignment between *Rb. sphaeroides* and *Cf. aurantiacus* RC sequences shows that W196(L) and W174(M) in *Cf. aurantiacus* are analogous to W156(L) and W185(M) in *Rb. sphaeroides* RCs,[21] which suggests that these two conserved tryptophans may also serve as probes in measuring the protein dynamics in *Cf. aurantiacus* RCs.[30] The tryptophan absorbance kinetic changes from Q_A^--depleted *Cf. aurantiacus* RCs are compared with those from Q_A^--depleted *Rb. sphaeroides* RCs over 350 ps in Figure 2. The protein relaxation in Q_A^--depleted *Cf. aurantiacus* RCs appears to have a larger amplitude contribution from the slow component than what is observed in *Rb. sphaeroides* RCs during the first 50 ps. Thus, the overall decay rate of the tryptophan absorbance change is slower in *Cf. aurantiacus* than in *Rb. sphaeroides*, even though the actual time constant of the slow component in Cf. aurantiacus is shorter than that in *Rb. sphaeroides* RCs. Previous resonance Raman measurements by Cherepy et al. showed a frequency downshift in the low-frequency (29−100 cm^{-1}) region of the special pair in *Cf. aurantiacus* RCs as compared with *Rb. sphaeroides* RCs.[35] The small frequency downshift can be interpreted as porphyrin ring core size expansion due to an increase in the low-frequency anharmonic vibrations of the protein,[36,37] which is consistent with the observation of the increased weight of the slow protein diffusion kinetic components in the *Cf. aurantiacus* RC.

Temperature Dependence of the Initial Electron Transfer in *Cf. aurantiacus* versus *Rb. sphaeroides* RCs. The only transient absorption study of the temperature-dependent kinetics of initial electron transfer in *Cf. aurantiacus* RCs was performed in 1991 using Q_A-containing RCs embedded in polyvinyl alcohol films between 80 and 320 K.[22] A 10 Hz laser was used to avoid the accumulation of closed RCs in the sample and excitation was at 605 nm. At that time, it was not possible to excite P directly in the near IR, and the time resolution of the instrument was limited to about a picosecond. The P* decay kinetics at room temperature (296 K), when fit to a single exponential decay term, gave a lifetime of 7.1 ps. At 320 K, the single exponential lifetime increased slightly to 9.0 ps. The kinetics measured over most of the temperature range were clearly heterogeneous, with biexponential fits at 80 K giving lifetimes of about 2 and 23 ps. Stretched-exponential fitting of the decay as a function of temperature suggested that above 200 K, the kinetics approached single exponential. The only temperature-dependent studies performed below 80 K used the fluorescence decay to estimate the electron transfer kinetics.[38] In this case, the RCs were in the state PQ_A^-, generated by white light illumination in the presence of an electron donor to rereduce P. The measurements under these conditions gave much longer times for P* decay, with two time constants of 20 and 300 ps, possessing a 1:1 amplitude ratio and exhibiting a very weak temperature dependence over the measured range.

In order to better understand the temperature-dependent kinetics of electron transfer in *Cf. aurantiacus*, and be able to compare it in detail to that of *Rb. sphaeroides*, transient absorbance measurements of quinone-depleted RCs were performed between 10 and 294 K exciting directly into the Q_Y band of P at 860 nm. Current ultrafast spectroscopic equipment not only allows direct excitation of P, but provides a much higher time resolution and much greater signal-to-noise ratios using much lower excitation energy. Figure 3 shows the P* stimulated emission decay kinetics at 930 nm on a 40-ps time scale at selected temperatures. The solid lines result from two-exponential fits of the data (discussed in the following paragraph). The P* kinetics of Q_A-depleted *Rb. sphaeroides* RCs were also measured using the same protocol (see below). For *Cf. aurantiacus* RCs, at least two exponential components and a nondecaying component are required to describe the kinetics at early times (<40 ps) over the entire temperature range measured. This model provides a qualitatively accurate kinetic picture during the first 40 ps and will be used to compare the kinetics of *Cf. aurantiacus* versus *Rb. sphaeroides* RCs at early times as a function of temperature. However, measurements over longer time periods clearly show more complex kinetic heterogeneity that is best described with the sum of two stretched-exponentials. In the following analyses, the results from fits using two exponential components plus a

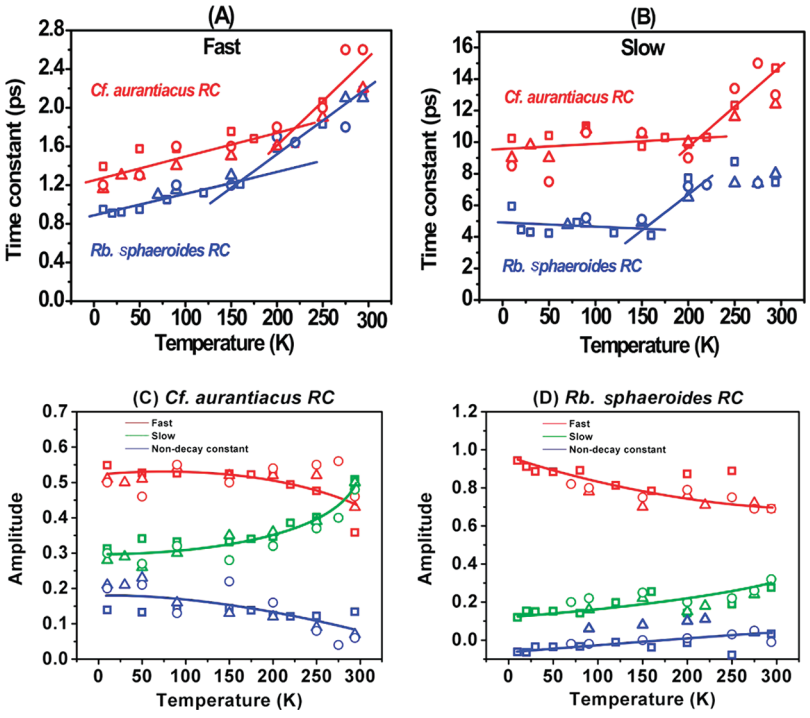

Figure 4. Decay lifetimes and relative amplitudes of P* decay kinetics as a function of temperature, obtained from fitting over the first 40 ps kinetics using two exponential components and a nondecaying term. Decay lifetimes of the (A) fast and (B) slow components as a function of temperature. Red represents *Cf. aurantiacus* RCs, blue represents *Rb. sphaeroides* RCs. The amplitude of each component as a function of temperature: (C) *Cf. aurantiacus* RCs; (D) *Rb. sphaeroides* RCs. The experiments were repeated three times for each (represented by square, triangle, and circle symbols, respectively).

nondecaying term (based on 40-ps kinetics traces) will first be presented, as this allows a simple way of understanding the overall temperature dependence of the early time kinetics. Then, the results from using a two-component stretched-exponential fit (based on 350-ps kinetics traces) will be analyzed. This provides a means of understanding the temperature and species dependence of the kinetic heterogeneity, as the β term is a measure of the width in the distribution of kinetic components.

Figure 4A,B shows P* decay lifetimes as a function of temperature, obtained from a fit with two exponential decay components and a nondecaying term for Q_A-depleted RCs of both *Cf. aurantiacus* and *Rb. sphaeroides*. At all temperatures, the fast-decaying lifetime for *Cf. aurantiacus* RCs is between 1 and 2 ps (3 ps in buffer without cryoprotectant at room temperature), while the slow lifetime varies between 10 and 15 ps. The fast-decay time constant gradually increases as the temperature is raised from 10 K to about 220 K, then a steeper increase occurs at 220 K. The slow-decay time constant does not show significant change in the 10 to 220 K region before a sharp increase occurs at 220 K. Similar shifts in the electron transfer rate constants occur in *Rb. sphaeroides* RCs, most clearly in the longer component lifetime, at around 160 K. The temperature range at which a sharp rate change takes place is similar to other studies that have investigated the temperature dependence of the atomic mean square displacement in protein and polymer systems,[39,40] referred to as the dynamic transition temperature or the dynamic crossover temperature. The current view on this phenomenon is that it is related to the β-relaxation processes of the protein hydration layer,[41] and a phenomenological explanation is an abrupt increase in the protein conformational entropy with increasing temperature, where the molecular collective motion converts from harmonic to anharmonic, mostly driven by the solvent interactions. Many thermodynamic quantities will correspondingly experience a transition at this temperature (e.g., reorganizational energy[42]).

Figure 4C,D compares the relative amplitudes of each kinetic component of the two samples and their temperature dependence. The amplitude of the fast component from *Rb. sphaeroides* RCs dominates at all temperatures below 250 K and shows little temperature dependence. The amplitude ratio of the fast to slow components decreased from 7.8:1 at low temperatures to 2.5:1 at room temperature. A similar biexponential decay of P* kinetics has been observed in RCs from other species of purple bacteria.[43−45] In *Cf. aurantiacus* RCs, the contribution from the slow component at all temperatures is significantly higher than that observed in *Rb. sphaeroides*. The amplitude ratio between the fast and slow components decreases from 1.75:1 to 0.7:1 as the temperature increases from 10 to 295 K, crossing 1 at around 250 K. The amplitudes of the kinetic components are not extremely temperature dependent.

As mentioned above, at low temperatures, the nonexponential character of the P* kinetics is particularly pronounced in *Cf. aurantiacus* RCs, with obvious decay kinetics extending beyond the 40 ps range. In the double-exponential analyses above, this long-lived component was treated as a nondecaying component and accounted for 10−15% of the overall amplitude. A two-component, stretched-exponential function allows the long decay components to be incorporated into the stretch index parameter for explicit consideration. We applied this method to the analysis of P* kinetics in *Cf. aurantiacus* RCs over a 350 ps time window. Figure 5 shows the variation of the stretched-exponential parameters with temperature. The stretch index (β) of the fast component (Figure 5A), starts near 0.8 at room temperature and gradually approaches 1 at temperatures below 90 K, suggesting that this fast decay process can be fairly well-described by a single relaxation process at all temperatures and a

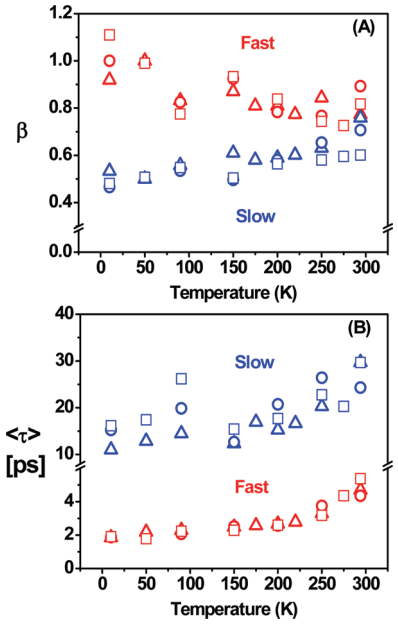

Figure 5. Two-component stretched-exponential fit performed on the 350 ps P* decay kinetics traces of *Cf. aurantiacus* RCs measured at all temperatures. (A) Stretched-exponential indices, β, as a function of temperature. (B) The average lifetime constants, $\langle\tau\rangle$, calculated using the formula described in the Material and Methods section.

nearly pure single exponential process at very low temperature. The narrowing in the kinetic distribution below 90 K is likely due to a limited protein nuclear diffusion along the electron transfer reaction coordinate on the ps time scale (average lifetime, τ, is 1−2 ps). For such short time periods, the protein motion is dominated by high-frequency covalent bond vibration and hydrogen bond fluctuation, leading to a quasi-harmonic coupling between these motions and the electron transfer reaction. In contrast, the slow component is more dispersive. Since the β parameters of both the fast and the slow stretched exponentials approach 1 at room temperature, it may be reasonable to model the room temperature electron transfer rate as biexponential. However, the stretch index of the slow component drops from 0.76 (at room temperature) to 0.5 (at 10 K), suggesting an increasingly dispersive lifetime distribution with decreasing temperature. The dispersive nature of the kinetics may be associated with conformational trapping at low temperatures, and more long-lived P* relaxation processes.

DISCUSSION

Temperature-Dependent Kinetics in RCs from *Cf. aurantiacus* and *Rb. sphaeroides*. While there are substantial structural and functional similarities between the RCs of *Cf. aurantiacus* and *Rb. sphaeroides*, there are clearly detailed differences in the spectrum and the charge separation process. Perhaps the most obvious structural difference is that the B_B cofactor in *Rb. sphaeroides* is replaced with a bacteriopheophytin in *Cf. aurantiacus*. However, the cofactor swap is clearly not the whole story, and may not be the most important difference functionally. This can be seen by considering the *Rb. sphaeroides* mutant M182HL in which B_B has been replaced with a bacteriopheophytin, resulting in the same cofactor composition as in *Cf. aurantiacus*.[46] Interestingly, the ground state absorbance spectra of the M182HL mutant and the *Cf. aurantiacus* RC are quite different. The Q_y absorption band of the newly introduced BPheo in the M182HL mutant is located at 785 nm, close to the accessory BChl absorption, while in *Cf. aurantiacus* RCs, the Q_y absorption band of all three BPheo cofactors peak near 756 nm. At room temperature, 35% of the electron transfer occurs along the B-branch in the M182HL mutant, while electron transfer in *Cf. aurantiacus* RCs apparently occurs almost exclusively along the A-branch at all temperatures.[47] All of these phenomena suggest that the detailed protein environment is functionally quite different between the two organisms. Recently, Pudlak and his coworkers used a five-site kinetic model to numerically simulate the electron transfer behavior of the two branches between *Rb. sphaeroides* and *Cf. aurantiacus* RCs.[48] The results suggest that a different mechanism of the unidirectional electron transfer exists in the two organisms.

The temperature dependence of the electron transfer kinetics in *Rb. sphaeroides* RCs and *Cf. aurantiacus* RCs differs in several ways. A biexponential analysis of the early time data (tens of picoseconds) shows that both RCs have a fast component lifetime of 1−3 ps and then a longer lifetime in the 4−15 ps range depending on the species and the temperature (Figure 4). The electron transfer is, overall, faster in *Rb. sphaeroides* RCs than in *Cf. aurantiacus* at any temperature. This is because in *Rb. sphaeroides* the contribution from the fast component dominates the overall electron transfer kinetics. In contrast, the amplitudes of the fast and slow decay components in *Cf. aurantiacus* RCs are more comparable at all temperatures and the slow component actually dominates near physiological temperature. The temperature at which there is a sharp change in the kinetics of electron transfer also differs between *Rb. sphaeroides* and *Cf. aurantiacus RCs*. This transition occurs at a higher temperature (∼220 K for both the fast and the slow components) for *Cf. aurantiacus* RCs than it does in *Rb. sphaeroides* RCs (∼150 K for the slow component and a less obvious transition between 100 and 150 K for the fast component).

It has been known for many years that *Rb. sphaeroides* RCs undergo protein conformational changes associated with charge separation and that some of those changes depend strongly on temperature,[49,50] with the most pronounced changes occurring near 150 K. In addition, resonance Raman spectroscopy has indicated relatively sharp changes in specific vibrational modes in a similar temperature range.[51,52] The temperature dependence of electron transfer in *Rhodopseudomona (Rp.) viridis* and *Rb. capsulatus* RCs (both mesophillic organisms) indicates a transition temperature very similar to that seen in *Rb. sphaeroides*.[44,53,54]

Multiple types of protein−protein and protein cofactor interactions may be involved in controlling the transition temperature in the electron transfer kinetics. A comparison between the RC amino acid sequences of the two species suggests that *Cf. aurantiacus* RCs may have fewer hydrogen bonding interactions with their cofactors than do *Rb. sphaeroides* RCs. In particular, glutamic acid L104, which hydrogen bonds to H_A, and histidine L168, which forms a hydrogen bond with P_A in *Rb. sphaeroides*, are glutamine and phenylalanine, respectively, in *Cf. aurantiacus*. The vibrational relaxation properties of BChl *a* in solution apparently depend on the hydrogen-bonding capability of the solvent,[55] again consistent with the idea that specific hydrogen bonds may affect the vibrational coupling associated with BChl *a* on the nanosecond time scale and further change its temperature-dependent behavior.

In addition to specific protein/cofactor interactions, temperature-dependent changes in the dielectric nature of the protein

Table 1. Amino Acid Compositions from Various RCs[a]

		Cf. aurantiacus J-10-fl RC	*Rb. sphaeroides* 2.4.1 RC	*Rp. viridis* RC	*Rb. capsulatus* SB 1003 RC
L branch	number of positively charged residues (+)	24	14	16	14
	number of negatively charged residues (−)	20	14	14	13
	aliphatic index	85.27	102.45	97.88	93.05
	grand average of hydropathy	0.286	0.586	0.468	0.551
M branch	number of positively charged residues (+)	18	17	19	20
	number of negatively charged residues (−)	15	14	18	14
	aliphatic index	91.27	94.45	88.61	90.00
	grand average of hydropathy	0.333	0.436	0.342	0.394

[a] Statistics are assembled by the ProtParam module from the ExPASy proteomics server.

environment can affect the overall electron transfer kinetics. Recent molecular dynamics simulations of the *Rb. sphaeroides* RC, as well as the small electron carrier plastocyanin, have suggested that the dynamic columbic interactions between proteins and local solvent molecules on the protein surface may play an important role in determining temperature-dependent changes in the dynamic behavior of the protein and its immediate solvent shell transitions.[42,56] The amino acid composition of *Cf. aurantiacus* RCs is compared with three RCs from purple bacteria in Table 1. Generally speaking, the *Cf. aurantiacus* RCs contain more charged residues and fewer aliphatic residues, especially in the L subunit. Sequence alignment (http://blast.ncbi.nlm.nih.gov/) and structural comparison indicate that 10 out of the 14 non-charged-to-charged residue changes from *Rb. sphaeroides* to *Cf. aurantiacus* RCs in the L-subunit are located at the periplasmic membrane surface. These charged residues presumably form ion pairs and optimize the surface electrostatic interactions (both protein/protein and protein/solvent) to stabilize the structure at high temperature, as has been seen in other thermophilic proteins.[57]

Dipole reorientation at the protein−water interface appears to be a critical factor in inducing the protein structural fluctuation, especially at higher temperatures.[58] The nondecaying component that results from a double exponential analyses or *Cf. aurantiacus* RC kinetics has a lifetime of 100−200 ps, which is comparable to the bulk protein electrostatic relaxation lifetime that has been estimated for *Rb. sphaeroides* RCs.[59] This is also consistent with the observation of a more distinct temperature transition for the slow component from a two exponential analysis (Figure 4b). The effect of dynamics at the protein−water interface is necessarily less on the picosecond time scale, as this is too fast for most collective protein motions, but the temperature-dependent transition in the kinetics is still apparent. In addition to the protein surface differences between *Cf. aurantiacus* and *Rb. sphaeroides* RCs discussed above, the lack of an H-subunit in *Cf. aurantiacus* RCs may also result in more direct exposure of protein surfaces to water in comparison with *Rb. sphaeroides* RCs, increasing solvent associated effects.

Using the Reaction Diffusion Model to Explore Electron Transfer Parameters at Room Temperature. In *Rb. sphaeroides* RCs, it has been previously shown that the detailed electron transfer kinetics can be accurately represented using a reaction diffusion model in which protein dynamics controls the rate of electron transfer.[30] This model contains several important parameters including the electronic coupling, the driving force, the time-dependent conformational diffusion, and fast and slow

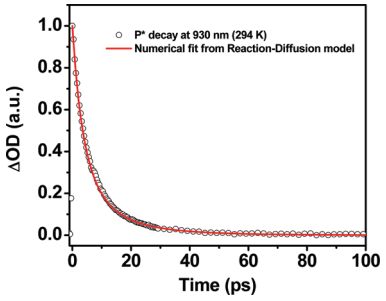

Figure 6. A fit of the P* decay in *Cf. aurantiacus* RCs monitored at 930 nm (circle) using the reaction diffusion model.[31] All of the parameters used in the fit were either experimentally derived from independent measurements or taken from the fitting parameters previously determined for *Rb. sphaeroides* (see Materials and Methods).

reorganization energy. The surprising thing about the application of this model to *Rb. sphaeroides* RCs is that it was possible to describe the complex and widely varying kinetics of a large number of mutants that specifically changed the driving force for electron transfer by varying only that parameter between mutants.

One question is whether that analysis can be extended to *Cf. aurantiacus* RCs, and if so, which parameters will change and which will remain the same. Two of the parameters can be obtained from experimental data. Volk and co-workers used magnetic field-dependent reaction yield measurements to estimate the standard free energy gap between P* and $P^+H_A^-$ for the RCs of both *Rb. sphaeroides* and *Cf. aurantiacus*. They found that the driving force for *Cf. aurantiacus* RCs was 0.04 eV lower than that of *Rb. sphaeroides* RCs.[27] Thus, for the analysis below, the driving force for *Cf. aurantiacus* RCs will similarly be set 0.04 eV below the value previously determined in modeling *Rb. sphaeroides* RCs (0.197 eV). In addition, the measured Trp decay for *Cf. aurantiacus* RCs (Figure 2) will be used to derive the time-dependent diffusion term, as described previously.[30] All other parameters will be held as they were in *Rb. sphaeroides*.

Fixing these two parameters at their measured values and changing nothing else results in essentially perfect simulation of the room temperature *Cf. aurantiacus* kinetics for the first 100 ps (Figure 6). One might have expected that the reorganization energies associated with the initial electron transfer in *Cf. aurantiacus* RC would have been substantially different from those of *Rb. sphaeroides*. However, comparisons between them using coherence spectroscopy in the Ba-absorbance region at

90 K,[60] and also the resonance Raman spectra at room temperature[35] have suggested that distribution of intramolecular motions that likely contribute to the reorganization energy on this time scale are actually quite similar between the two organisms. In practice, the two reorganization energies can be varied by about 0.02 eV before the fit deviates significantly from the data.

■ ASSOCIATED CONTENT

Supporting Information. Figures S1−S3 provide additional spectroscopic data for Q_A-containing and Q_A-depleted *Cf. aurantiacus* RCs. A mathematical form of the reaction-diffusion model for electron transfer is also provided. This material is available free of charge via the Internet at http://pubs.acs.org.

■ AUTHOR INFORMATION

Corresponding Author

*E-mail: nwoodbury@asu.edu.

Present Addresses

[§]College of Life Sciences, HangZhou Normal University, HangZhou, China.

[∥]State Key Laboratory on Integrated Optoelectronics, College of Electronic Science and Engineering, Jilin University, 2699 Qianjin Street, Changchun 130012, China.

■ ACKNOWLEDGMENT

We thank Dr. Dmitry Matyushov for helpful discussions. This work was funded by NSF grants MCB-0642260 to the ASU group and MCB-0646621 to R.E.B. H.Y.W. was supported in part by NSF China Grant 20973081.

■ REFERENCES

(1) Bryngelson, J. D.; Onuchic, J. N.; Socci, N. D.; Wolynes, P. G. *Proteins: Struct., Funct., Bioinf.* **1995**, *21*, 167–195.

(2) Chan, H. S.; Dill, K. A. *Proteins: Structure, Function, and Bioinformatics* **1998**, *30*, 2–33.

(3) Duan, Y.; Kollman, P. A. *Science* **1998**, *282*, 740–744.

(4) Klepeis, J. L.; Lindorff-Larsen, K.; Dror, R. O.; Shaw, D. E. *Current Opinion in Structural Biology* **2009**, *19*, 120–127.

(5) Chandler, D. E.; Hsin, J.; Harrison, C. B.; Gumbart, J.; Schulten, K. *Biophys. J.* **2008**, *95*, 2822–2836.

(6) Groenhof, G.; Bouxin-Cademartory, M.; Hess, B.; de Visser, S. P.; Berendsen, H. J. C.; Olivucci, M.; Mark, A. E.; Robb, M. A. *J. Am. Chem. Soc.* **2004**, *126*, 4228–4233.

(7) Xie, X. S. *J. Chem. Phys.* **2002**, *117*, 11024–11032.

(8) Neuweiler, H.; Sauer, M. *Curr. Pharm. Biotechnol.* **2004**, *5*, 285–298.

(9) Hofmann, C.; Aartsma, T. J.; Michel, H.; Köhler, J. *Proc. Natl. Acad. Sci. U.S.A.* **2003**, *100*, 15534–15538.

(10) Hellingwerf, K. J.; Hendriks, J.; Gensch, T. *J. Phys. Chem. A* **2003**, *107*, 1082–1094.

(11) Birge, R. R. *Annu. Rev. Phys. Chem.* **1990**, *41*, 683–733.

(12) Gai, F.; Hasson, K. C.; McDonald, J. C.; Anfinrud, P. A. *Science* **1998**, *279*, 1886–1891.

(13) Andel, F.; Lagarias, J. C.; Mathies, R. A. *Biochemistry* **1996**, *35*, 15997–16008.

(14) Chapman, H. N.; Fromme, P.; Barty, A.; White, T. A.; Kirian, R. A.; Aquila, A.; Hunter, M. S.; Schulz, J.; DePonte, D. P.; Weierstall, U.; et al. *Nature* **2011**, *470*, 73–77.

(15) Schotte, F.; Lim, M.; Jackson, T. A.; Smirnov, A. V.; Soman, J.; Olson, J. S.; Phillips, G. N.; Wulff, M.; Anfinrud, P. A. *Science* **2003**, *300*, 1944–1947.

(16) Ihee, H.; Rajagopal, S.; Šrajer, V.; Pahl, R.; Anderson, S.; Schmidt, M.; Schotte, F.; Anfinrud, P. A.; Wulff, M.; Moffat, K. *Proc. Natl. Acad. Sci. U.S.A.* **2005**, *102*, 7145–7150.

(17) Blankenship, R. E.; Feick, R.; Bruce, B. D.; Kirmaier, C.; Holten, D.; Fuller, R. C. *J. Cell. Biochem.* **1983**, *22*, 251–261.

(18) Pierson, B. K.; Thornber, J. P. *Proc. Natl. Acad. Sci.* **1983**, *80*, 80–84.

(19) Holzwarth, A. R.; Muller, M. G. *Biochemistry* **1996**, *35*, 11820–11831.

(20) Pierson, B.;Castenholz, R. *The Prokaryotes—A Handbook on the Biology of Bacteria: Ecophysiology, Isolation, Identification, Applications*; Springer-Verlag: Berlin, Heidelberg, and New York, 1992; pp 3754−3774.

(21) Ovchinnikov, Y. A.; Abdulaev, N. G.; Shmuckler, B. E.; Zargarov, A. A.; Kutuzov, M. A.; Telezhinskaya, I. N.; Levina, N. B.; Zolotarev, A. S. *FEBS Lett.* **1988**, *232*, 364–368.

(22) Becker, M.; Nagarajan, V.; Middendorf, D.; Parson, W. W.; Martin, J. E.; Blankenship, R. E. *Biochim. Biophys. Acta* **1991**, *1057*, 299–312.

(23) Kirmaier, C.; Holten, D. *Photosynth. Res.* **1987**, *13*, 225–260.

(24) Woodbury, N.; Allen, J. The Pathway, Kinetics and Thermodynamics of Electron Transfer in Wild Type and Mutant Reaction Centers of Purple Nonsulfur Bacteria. In *Anoxygenic Photosynthetic Bacteria*; Blankenship, R. E.Madigan, M. T.Bauer, C. E., Eds.; Kluwer Academic Publishers: Dordrecht, The Netherlands, 1995; Chapter 24, pp 527−557.

(25) Du, M.; Rosenthal, S. J.; Xie, X.; DiMagno, T. J.; Schmidt, M.; Hanson, D. K.; Schiffer, M.; Norris, J. R.; Fleming, G. R. *Proc. Natl. Acad. Sci. U.S.A.* **1992**, *89*, 8517–8521.

(26) Kirmaier, C.; Blankenship, R. E.; Holten, D. *Biochim. Biophys. Acta, Bioenerg.* **1986**, *850*, 275–285.

(27) Volk, M.; Aumeier, G.; Langenbacher, T.; Feick, R.; Ogrodnik, A.; Michel-Beyerle, M. E. *J. Phys. Chem. B* **1998**, *102*, 735–751.

(28) Collins, A. M.; Kirmaier, C.; Holten, D.; Blankenship, R. E. *Biochim. Biophys. Acta, Bioenerg.* **2011**, *1807*, 262–269.

(29) Xin, Y. Y.; Lin, S.; Blankenship, R. E. *J. Phys. Chem. A* **2007**, *111*, 9367–9373.

(30) Wang, H.; Lin, S.; Allen, J. P.; Williams, J. C.; Blankert, S.; Laser, C.; Woodbury, N. W. *Science* **2007**, *316*, 747–750.

(31) Wang, H. Y.; Lin, S.; Katilius, E.; Laser, C.; Allen, J. P.; Williams, J. C.; Woodbury, N. W. *J. Phys. Chem. B* **2009**, *113*, 818–824.

(32) Hamm, P.; Gray, K. A.; Oesterhelt, D.; Feick, R.; Scheer, H.; Zinth, W. *Biochim. Biophys. Acta, Bioenerg.* **1993**, *1142*, 99–105.

(33) Woodbury, N. W.; Parson, W. W.; Gunner, M. R.; Prince, R. C.; Dutton, P. L. *Biochim. Biophys. Acta, Bioenerg.* **1986**, *851*, 6–22.

(34) Woodbury, N. W. T.; Parson, W. W. *Biochim. Biophys. Acta, Bioenerg.* **1984**, *767*, 345–361.

(35) Cherepy, N. J.; Holzwarth, A. R.; Mathies, R. A. *Biochemistry* **1995**, *34*, 5288–5293.

(36) Dasgupta, S.; Spiro, T. G.; Johnson, C. K.; Dalickas, G. A.; Hochstrasser, R. M. *Biochemistry* **1985**, *24*, 5295–5297.

(37) Asher, S. A.; Murtaugh, J. *J. Am. Chem. Soc.* **1983**, *105*, 7244–7251.

(38) Schweitzer, G.; Hucke, M.; Griebenow, K.; Muller, M. G.; Holzwarth, A. R. *Chem. Phys. Lett.* **1992**, *190*, 149–154.

(39) Doster, W.; Cusack, S.; Petry, W. *Nature* **1989**, *337*, 754–756.

(40) Dechter, J. J.; Axelson, D. E.; Dekmezian, A.; Glotin, M.; Mandelkern, L. *J. Polym. Sci.: Polym. Phys. Ed.* **1982**, *20*, 641–650.

(41) Frauenfelder, H.; Chen, G.; Berendzen, J.; Fenimore, P. W.; Jansson, H.; McMahon, B. H.; Stroe, I. R.; Swenson, J.; Young, R. D. *Proc. Natl. Acad. Sci. U.S.A.* **2009**, *106*, 5129–5134.

(42) LeBard, D. N.; Matyushov, D. V. *J. Phys. Chem. B* **2009**, *113*, 12424–12437.

(43) Hartwich, G.; Lossau, H.; Michel-Beyerle, M. E.; Ogrodnik, A. *J. Phys. Chem. B* **1998**, *102*, 3815–3820.

(44) Huppmann, P.; Arlt, T.; Penzkofer, H.; Schmidt, S.; Bibikova, M.; Dohse, B.; Oesterhelt, D.; Wachtveit, J.; Zinth, W. *Biophys. J.* **2002**, *82*, 3186–3197.

(45) Jia, Y.; DiMagno, T. J.; Chan, C. K.; Wang, Z.; Popov, M. S.; Du, M.; Hanson, D. K.; Schiffer, M.; Norris, J. R.; Fleming, G. R. *J. Phys. Chem.* **1993**, *97*, 13180–13191.

(46) Katilius, E.; Katiliene, Z.; Lin, S.; Taguchi, A. K. W.; Woodbury, N. W. *J. Phys. Chem. B* **2002**, *106*, 1471–1475.
(47) Volk, M.; Scheidel, G.; Ogrodnik, A.; Feick, R.; Michelbeyerle, M. E. *Biochim. Biophys. Acta* **1991**, *1058*, 217–224.
(48) Pudlak, M.; Pincak, R. *J. Biol. Phys.* **2010**, *36*, 273–289.
(49) Kleinfeld, D.; Okamura, M. Y.; Feher, G. *Biochemistry* **1984**, *23*, 5780–5786.
(50) Muh, F.; Williams, J. C.; Allen, J. P.; Lubitz, W. *Biochemistry* **1998**, *37*, 13066–13074.
(51) Peloquin, J. M.; Violette, C. A.; Frank, H. A.; Bocian, D. F. *Biochemistry* **1990**, *29*, 4892–4898.
(52) Ivancich, A.; Lutz, M.; Mattioli, T. A. *Biochemistry* **1997**, *36*, 3242–3253.
(53) Chan, C.-K.; X-Q Chen, L.; DiMagno, T. J.; Hanson, D. K.; Nance, S. L.; Schiffer, M.; Norris, J. R.; Fleming, G. R. *Chem. Phys. Lett.* **1991**, *176*, 366–372.
(54) Taguchi, A. K. W.; Lin, S.; Jackson, J. A.; Woodbury, N. W. *Biochemistry* **2000**, *39*, 14787–14798.
(55) Bellacchio, E.; Sauer, K. *J. Phys. Chem. B* **1999**, *103*, 2279–2290.
(56) LeBard, D. N.; Matyushov, D. V. *Phys. Rev. E* **2008**, *78*, 061901.
(57) Dominy, B. N.; Perl, D.; Schmid, F. X.; Brooks, C. L. *J. Mol. Biol.* **2002**, *319*, 541–554.
(58) Matyushov, D.;Morozov, A. *Arxiv preprint arXiv:1011.1023* 2010.
(59) LeBard, D. N.; Kapko, V.; Matyushov, D. V. *J. Phys. Chem. B* **2008**, *112*, 10322–10342.
(60) Yakovlev, A. G.; Vasilieva, L. G.; Shkuropatov, A. Y.; Bolgarina, T. I.; Shkuropatova, V. A.; Shuvalov, V. A. *J. Phys. Chem. A* **2003**, *107*, 8330–8338.
(61) Deisenhofer, J.; Epp, O.; Sinning, I.; Michel, H. *J. Mol. Biol.* **1995**, *246*, 429–457.